oxidized to the parent cluster. The cluster acts as an electron storage site through the reversible breakage and formation of metal–metal bonds, although the cycle is not 100% efficient. In general, the electrochemical results indicate that the rearrangement of the Bi–Fe clusters is very rapid on the electrode surface.

Acknowledgment. The National Science Foundation (Grant CHE-8421217) and the Robert A. Welch Foundation are to be thanked for their financial support of this research. The high-pressure equipment was purchased through a grant from the Atlantic Richfield Foundation, administered by the Research Corp.

Registry No. $[Et_4N]_2[\mathbf{1}]$, 101858-51-9; $[Me_4N]_2[\mathbf{1}]\cdot[Me_4N][Cl]$, 101834-85-9; $[Et_4N][\mathbf{2}]$, 101997-75-5; $[Et_4N]_3[Bi\{Fe(CO)_4\}_4]$, 92763-37-6; $[Et_4N]_2[Bi_4Fe_4(CO)_{13}]$, 94483-21-3; $Fe(CO)_5$, 13463-40-6; $Bi_2Fe_3(CO)_9$, 96525-96-1; $[Cu(CH_3CN)_4][BF_4]$, 15418-29-8; $[Fe(CO)_4]^{2-}$, 22321-35-3; $[Co(CO)_4]^-$, 14971-27-8; $Co_2(CO)_8$, 15226-74-1; $[Et_4N][BiFe_3(CO)_{10}]$, 92786-73-7; Cp_2Co, 1277-43-6; $[Cp_2Co]_2[Bi_2Fe_3(CO)_9]$, 109243-26-7; $(Bi_2Fe_3(CO)_9)^-$, 109243-27-8; Bi, 7440-69-9; Co, 7440-48-4; Fe, 7439-89-6.

Supplementary Material Available: For $[Me_4N]_2[\mathbf{1}]\cdot[Me_4N][Cl]$ and $[Et_4N][\mathbf{2}]$ listings of anisotropic thermal parameters, Figures 2 and 4 (stereoviews of the anions $[\mathbf{1}]^{2-}$ and $[\mathbf{2}]^-$), and tables of bond length and angle parameters for the cations of $[Me_4N]_2[\mathbf{1}]\cdot[Me_4N][Cl]$ and $[Et_4N][\mathbf{2}]$ (5 pages); tables of calculated and observed structure factors for both compounds (43 pages). Ordering information is given on any current masthead page.

Contribution from the Department of Chemistry, University of South Carolina, Columbia, South Carolina 29208

Cluster Syntheses. 14. The Syntheses and Structural Characterizations of the High-Nuclearity Sulfidoruthenium Carbonyl Cluster Compounds $Ru_5(CO)_{14}(\mu_4\text{-}S)_2$, $Ru_6(CO)_{17}(\mu_4\text{-}S)_2$, and $Ru_7(CO)_{20}(\mu_4\text{-}S)_2$

Richard D. Adams,* James E. Babin, and Miklos Tasi

Received February 3, 1987

The reaction of $Ru_3(CO)_9(\mu_3\text{-}S)_2$ (**2**) with $Ru_3(CO)_{12}$ under UV irradiation has yielded the higher nuclearity cluster compounds $Ru_4(CO)_9(\mu\text{-}CO)_2(\mu_4\text{-}S)_2$ (**3**), 38%, $Ru_5(CO)_{14}(\mu_4\text{-}S)_2$ (**4**), 20%, and $Ru_6(CO)_{17}(\mu_4\text{-}S)_2$ (**5**), 3%. Thermal decarbonylation of $Ru_3(CO)_9(\mu_3\text{-}CO)(\mu_3\text{-}S)$ (**1**) at 100 °C has yielded **3**, 47%, **5**, 10%, and $Ru_7(CO)_{20}(\mu_4\text{-}S)_2$ (**6**), 26%. The large clusters are decomposed to **2** and **3** by reaction with CO at 1 atm. Compounds **4–6** have been characterized by single-crystal X-ray diffraction analyses. For **4**: space group $P2_1/n$, a = 8.787 (2) Å, b = 14.550 (3) Å, c = 19.741 (3) Å, β = 98.09 (1)°, Z = 4, ρ_{calcd} = 2.56 g/cm^3. The structure was solved by direct methods and was refined (3023 reflections) to the final residuals R_F = 0.033 and R_{wF} = 0.036. The cluster consists of an approximately square arrangement of four ruthenium atoms with quadruply bridging sulfido ligands on each face. An $Ru(CO)_4$ unit bridges one Ru–Ru edge of the cluster. By the EAN rule the molecule is unsaturated, and one of the Ru–Ru bonds was found to be unusually short, 2.704 (1) Å. For **5**: space group $P2_12_12_1$, a = 11.211 (2) Å, b = 14.666 (4) Å, c = 17.611 (4) Å, Z = 4, ρ_{calcd} = 2.63 g/cm^3. Compound **5** is isomorphous and isostructural with the known osmium homologue. The structure was refined (2482 reflections) to the final values of the residuals R_F = 0.033 and R_{wF} = 0.039. The molecule consists of a pentagonal-bipyramidal cluster of five ruthenium atoms with two sulfido ligands. A $Ru(CO)_4$ group bridges one apical–equatorial edge of the cluster. For **6**: space group $P2_12_12_1$, a = 11.226 (3) Å, b = 14.320 (4) Å, c = 21.217 (5) Å, Z = 4, ρ_{calcd} = 2.59 g/cm^3. Compound **6** is isomorphous and isostructural with the known osmium homologue. The structure was refined (2296 reflections) to the final values of the residuals R_F = 0.041 and R_{wF} = 0.044. The molecule consists of a pentagonal-bipyramidal cluster of five ruthenium atoms and two sulfido ligands. Two $Ru(CO)_4$ groups bridge symmetrically adjacent apical–equatorial edges of the cluster. The chemistry of the ruthenium clusters is compared to that of the corresponding osmium system.

Introduction

A number of methods have now been developed for the systematic synthesis of transition-metal cluster compounds.[1,2] Bridging ligands have been shown to be especially useful by facilitating metal atom addition reactions and by stabilizing the products.[1-4] Bridging ligands appear to play an important role in the chemistry of high-nuclearity clusters of ruthenium.[5] No neutral binary carbonyls containing more than three ruthenium atoms are known.[6]

We have had considerable success in our efforts to prepare high-nuclearity cluster compounds of osmium containing sulfido ligands[3] and have now begun to apply this knowledge to the development of the chemistry of sulfidoruthenium carbonyl clusters. We have recently reported high-yield syntheses of the sulfidotriruthenium carbonyl clusters $Ru_3(CO)_9(\mu_3\text{-}CO)(\mu_3\text{-}S)$ (**1**) and $Ru_3(CO)_9(\mu_3\text{-}S)_2$ (**2**) from the reaction of $Ru_3(CO)_{12}$ with ethylene sulfide.[7]

Experimental Section

General Information. Reagent grade solvents were stored over 4-Å molecular sieves. THF was freshly distilled from sodium diphenylketyl before use. $Ru_3(CO)_{12}$ was purchased from Strem Chemical Co. and was used as received. Ethylene sulfide was purchased from Aldrich Chemical Co. and was distilled before use. CP grade carbon monoxide was purchased from Linde Co. and was used without further purification. $Ru(CO)_5$ was prepared by the literature methods.[8] $Ru_3(CO)_9(\mu_3\text{-}CO)(\mu_3\text{-}S)$ (**1**), $Ru_3(CO)_9(\mu_3\text{-}S)_2$ (**2**), and $Ru_4(CO)_9(\mu\text{-}CO)_2(\mu_4\text{-}S)_2$ (**3**) were prepared as previously reported.[7]

All reactions were performed under a nitrogen atmosphere. All chromatographic separations were performed in air. TLC separations were performed on plates (0.25-mm Kieselgel 60 F_{254}, E. Merck) purchased from Bodman Chemicals. UV irradiation experiments were performed by using an external high-pressure mercury lamp on reaction solutions contained in Pyrex glassware. IR spectra were recorded on a Nicolet 5 DXB FT IR spectrometer. Elemental analyses were performed by MicAnal, Tucson, AZ.

(1) Geoffroy, G. L. In *Comprehensive Organometallic Chemistry*; Wilkinson, G., Stone, F. G. A., Abel, E., Eds., Pergamon: Oxford, England, 1982; Chapter 40.
(2) Geoffroy, G. L. In *Metal Clusters in Catalysis*; Gates, B. C., Guczi, L., Knözinger, H., Eds.; Elsevier: New York, 1986.
(3) Adams, R. D. *Polyhedron* **1985**, *4*, 2003.
(4) Vahrenkamp, V., *Philos. Trans. R. Soc. London, A* **1982**, *308*, 17.
(5) Bruce, M. I. In *Comprehensive Organometallic Chemistry*; Wilkinson, G., Stone, F. G. A., Abel, E. W., Eds.; Pergamon: Oxford, England, 1982; Chapter 32.6.
(6) See ref 5, Chapter 32.2.1.4.
(7) Adams, R. D.; Babin, J. E.; Tasi, M. *Inorg. Chem.* **1986**, *25*, 4514.
(8) Huq, R.; Poë, A. J.; Charola, S. *Inorg. Chim. Acta* **1980**, *38*, 121.

0020-1669/87/1326-2807$01.50/0

Reaction of $Ru_3(CO)_9(\mu_3\text{-}S)_2$ (2) with $Ru_3(CO)_{12}$. A 31-mg (0.050-mmol) sample of compound **2** and 32 mg (0.050 mmol) of $Ru_3(CO)_{12}$ were dissolved in 70 mL of THF, and the solution was irradiated at 25 °C for 5 h under a continuous purge with N_2. The solution turned to dark green. The THF was removed in vacuo, and the residue was extracted with 150 mL of hexane. The gray-green hexane extract was concentrated and chromatographed on a short Florisil column with hexane solvent. The first yellow band was unreacted $Ru_3(CO)_{12}$, 9.7 mg (30%). The second band (dark green) that eluted with a hexane/CH_2Cl_2 v/v 8/2 solvent mixture was a mixture of $Ru_5(CO)_{14}(\mu_4\text{-}S)_2$ (**4**) and $Ru_6(CO)_{17}(\mu_4\text{-}S)_2$ (**5**). These were separated by fractional crystallization from a hexane solution at −20 °C. This yielded 9.4 mg (20%) of dark green **4** and 1.6 mg (3%) of brown **5**. IR (ν(CO), cm^{-1}; in hexane) for **4**: 2114 (w), 2075 (vs), 2049 (vs), 2032 (s), 2022 (s), 2007 (w), 1969 (m). Anal. Calcd for $Ru_5S_2O_{14}C_{14}$: C, 17.48. Found: C, 17.76. IR (ν(CO), cm^{-1}; in hexane) for **5**: 2113 (w), 2083 (vs), 2061 (vs), 2051 (s), 2046 (m, sh), 2029 (s), 2018 (w), 2009 (w), 1990 (vw), 1971 (vw), 1956 (w). Anal. Calcd for $Ru_6S_2O_{17}C_{17}$: C, 23.38. Found: C, 23.17. A dark orange residue that remained after the hexane extraction was further extracted with 50 mL of hot CH_2Cl_2. The solution was concentrated and cooled to −20 °C and yielded 14.7 mg of compound **3** (38%).

Reaction of 3 with $Ru_3(CO)_{12}$. A 40-mg (0.005-mmol) sample of compound **3** and 32 mg (0.05 mmol) of $Ru_3(CO)_{12}$ were dissolved in 80 mL of THF, and the solution was irradiated (UV) at 25 °C for 6 h under a purge with N_2. The color of the solution turned from orange to green. The workup described above resulted in 3.8 mg (8%) of compound **4**, 1.6 mg (3%) of compound **5**, and 28 mg (70%) of unreacted **3**.

Reaction of 4 with $Ru(CO)_5$. A 12-mg (0.0125-mmol) sample of compound **4** dissolved in 10 mL of cyclohexane was combined with a 50-mL solution of $Ru(CO)_5$ (0.073 mmol) in cyclohexane. This solution was irradiated (UV) for 10 h at 25 °C under a continuous purge with N_2. The dark green solution turned brown. The solution was concentrated and chromatographed on a Florisil column with hexane solvent. The first yellow band yielded 11.9 mg of $Ru_3(CO)_{12}$. A brown band eluted with a hexane/CH_2Cl_2 v/v 1/1 solvent mixture. This was further purified by TLC using a hexane/CH_2Cl_2 v/v 85/15 solvent mixture to yield 3.4 mg (24%) of brown **5** and 1.0 mg (5%) of brown **6**. IR (ν(CO), cm^{-1}; in hexane) for **6**: 2119 (w), 2097 (m), 2074 (s), 2056 (vs), 2033 (m), 2027 (m), 2018 (w, sh), 2014 (m), 1991 (vw), 1963 (vw, sh), 1957 (w). Anal. Calcd for $Ru_7S_2O_{20}C_{20}$: C, 18.03. Found: C, 18.06.

Attempted Preparation of 6 from Compound 5. An 8-mg (0.007-mmol) sample of **5** was dissolved in 10 mL of cyclohexane, and the mixture was combined with a 50-mL solution of $Ru(CO)_5$ (0.073 mmol) in cyclohexane. The solution was irradiated for 12 h at 25 °C under a purge with nitrogen. Separation on silica gel TLC plates using a hexane/CH_2Cl_2 v/v 8/2 solvent mixture yielded 15.2 mg of $Ru_3(CO)_{12}$ and 7.6 mg of unreacted **5**.

Thermolysis of $Ru_3(CO)_9(\mu_3\text{-}CO)(\mu_3\text{-}S)$ (1). (a) Under a CO Atmosphere. A 110-mg (0.18-mmol) sample of compound **1** was dissolved in 100 mL of heptane, and the solution was refluxed under a slow purge with carbon monoxide for 90 min. The yellow color of the solution turned brown. Approximately half of the solvent was removed in vacuo, and the solution was cooled to −20 °C. Orange crystals of **3** (16 mg, 23%) precipitated and were separated by filtration. The filtrate was chromatographed on a Florisil column with hexane eluent. This yielded a yellow band that was a mixture of compound **2** and $Ru_3(CO)_{12}$. These were separated by fractional crystallization from hexane solution. Yield: 17 mg of $Ru_3(CO)_{12}$ and 35 mg (62%) of compound **2**. By the use of a hexane/CH_2Cl_2 v/v 8/2 solvent mixture a brown band was eluted. Subsequent separation on TLC plates (hexane/CH_2Cl_2 v/v 8/2) yielded 4 mg of compound **6** (5%) and another brown compound, **7** (3 mg), which has not been fully characterized yet. IR (ν(CO), cm^{-1}; in hexane): 2083 (vs), 2060 (w), 2041 (m), 2033 (vw), 2029 (vw).

(b) Under Vacuum. A 70-mg (0.114-mmol) sample of **1** was placed into a thick-walled glass tube equipped with a magnetic stirrer, 8 mL of heptane was added, and the tube was sealed under vacuum. The tube was placed into an oil bath, and the solution was stirred vigorously at 100 °C for 10 min. After the tube was removed and cooled to 25 °C, an orange precipitate formed. The tube was opened, the solution was decanted, and the precipitate was extracted with CH_2Cl_2 several times. The undissolved residue was pure **3**, 21 mg (47%). The solutions were combined and evaporated to dryness. This residue was dissolved in hexane and was chromatographed on a Florisil column. With hexane eluent, a yellow band of 11 mg of $Ru_3(CO)_{12}$ was separated. A gray band of a mixture of **5** and **7** was eluted with a hexane/CH_2Cl_2 v/v 9/1 solvent mixture, and a brown band, compound **6**, was eluted with a hexane/CH_2Cl_2 v/v 7/3 solvent mixture (yield 14 mg, 26%). Separation of compounds **5** and **7** by TLC using a hexane/CH_2Cl_2 v/v 8/2 solvent mixture as eluent yielded 6.5 mg (10% of compound **5** and 2 mg of compound **7**.

Reaction of $Ru_4(CO)_9(\mu\text{-}CO)_2(\mu_4\text{-}S)_2$ (3) with CO. A 20-mg (0.026-mmol) sample of **3** was dissolved in 40 mL of CH_2Cl_2, and the solution was slowly purged with CO for 20 min at 25 °C. The solution was concentrated in vacuo and was chromatographed on TLC plates with hexane solvent. This yielded 14.7 mg of **2**, 92%.

Reaction of $Ru_5(CO)_{14}(\mu_4\text{-}S)_2$ (4) with CO. A 10-mg (0.010-mmol) sample of compound **4** was dissolved in 20 mL of hexane. While the solution was vigorously stirred, CO was bubbled through it at 25 °C for 15 min. The green solution became red, and an orange precipitate formed. Filtration separated 6.1 mg (76%) of compound **3**. The filtrate was evaporated to dryness in vacuo. The residue was dissolved in a minimum amount of CH_2Cl_2, and the solution was chromatographed by TLC using a hexane/CH_2Cl_2 v/v 7/3 solvent mixture. This yielded a major red band (2.2 mg). IR (ν(CO), cm^{-1}; in hexane): 2099 (m), 2077 (m), 2065 (vs), 2046 (m), 2009 (m), 1997 (w), 1983 (vw). Efforts to crystallize this complex were unsuccessful because in solution it was slowly (6–8 h) transformed into **3**.

Reaction of $Ru_6(CO)_{17}(\mu_4\text{-}S)_2$ (5) with CO. An 11-mg (0.0096-mmol) sample of **5** was dissolved in 20 mL of heptane. The solution was heated to reflux (98 °C) for 40 min under a CO purge. The brown solution became orange. Workup as described above yielded 5.2 mg (88%) of compound **2** and 0.7 mg (10%) of compound **3**. There was no evidence for the formation of **4**.

Reaction of $Ru_7(CO)_{20}(\mu_4\text{-}S)_2$ (6) with CO. The reaction of 10 mg (0.0075 mmol) of **6** with CO was performed as described in the previous section. No reaction occurred at 25 °C in 4 h, but at 98 °C **6** reacted completely in approximately 1 h. The usual workup yielded 3.5 mg of compound **2** (74%) and 0.7 mg of compound **3** (12%). There was no evidence for the formation of **4** or **5** under these conditions.

Thermolysis of 5. A 10-mg (0.009-mmol) sample of compound **5** was dissolved in 15 mL of heptane, and the solution was refluxed for 40 min under an N_2 atmosphere. The brown solution became orange, and workup as described above yielded 6 mg of compound **3** (90%).

Crystallographic Analyses. Dark green crystals of **4** and black crystals of **6** were grown by slow evaporation of solvent from hexane solutions at −20 °C and from benzene solutions at 25 °C, respectively. Black crystals of **5** were grown from a hexane/CH_2Cl_2 (9/1) solution at −20 °C. Data crystals were mounted in thin-walled glass capillaries. Diffraction measurements were made on a Rigaku AFC6 fully automated four-circle diffractometer using graphite-monochromatized Mo Kα radiation. Unit cells were determined and refined from 25 randomly selected reflections by using the AFC6 automatic search, index, center, and least-squares routines. Crystal data, data collection parameters, and results of the analyses are listed in Table I. All data processing was performed on a Digital Equipment Corp. MICROVAX II computer by using the Molecular Structure Corp. TEXSAN program library. Neutral-atom scattering factors were calculated by the standard procedures.[9a] Anomalous dispersion corrections were applied to all atoms.[9b] Full matrix least-squares refinements were minimized as indicated in Table I.

Compound **4** crystallized in the monoclinic crystal system. The space group $P2_1/n$ was determined from the systematic absences observed in the data. The positions of the metal atoms were determined by direct methods (MULTAN). All remaining atoms were located by subsequent difference Fourier syntheses. All atoms were refined with anisotropic thermal parameters.

Compounds **5** and **6** crystallized in the orthorhombic crystal system. The space group $P2_12_12_1$ was determined for both compounds by systematic absences observed in the data. Both compounds are isomorphous with the analogous osmium compounds, and structure solution for each was begun by placement of the metal and sulfur atoms at the same positions of the metal and sulfur atoms in the osmium clusters. All remaining atoms in these structures were determined by difference Fourier analyses. The data for compound **6** were corrected for the effects of absorption. Atoms larger than oxygen were refined with anisotropic thermal parameters. Attempts were made to determine the correct enantiomorph for both structures **5** and **6**. For compound **5** refinement of each enantiomer yielded the residuals $R_F = 0.0334$, $R_{wF} = 0.0385$ and $R_F = 0.0342$, $R_{wF} = 0.0394$. Although the results are not conclusive, the atomic coordinates for the enantiomer with the lower residuals were chosen to be correct (Table I). Similarly, refinement of both enantiomers of **6** yielded the residuals $R_F = 0.0412$, $R_{wF} = 0.0441$ and $R_F = 0.0495$, $R_{wF} = 0.0506$. In this case, the enantiomer with the lower residuals is surely the correct one. The fractional atomic coordinates for this enantiomer are reported. Error analyses were calculated from the inverse matrix obtained on the final cycle of refinement for each structure. See the supplementary material for the tables of structure factor amplitudes

(9) *International Tables for X-ray Crystallography*; Kynoch: Birmingham, England, 1975; Vol. IV: (a) Table 2.2B, pp 99–101; (b) Table 2.3.1, pp 149–150.

Table I. Crystallographic Data for the Structural Analyses of **4–6**

	4	**5**	**6**
	(A) Crystal Data		
formula	$Ru_5S_2O_{14}C_{14}$	$Ru_6S_2O_{17}C_{17}$	$Ru_7S_2O_{20}C_{20}$
temp (±3), °C	27	23	23
space group	$P2_1/n$, No. 14	$P2_12_12_1$, No. 19	$P2_12_12_1$, No. 19
a, Å	8.787 (2)	11.211 (2)	11.226 (3)
b, Å	14.550 (3)	14.666 (4)	14.320 (4)
c, Å	19.741 (3)	17.611 (4)	21.217 (5)
α, deg	90.0	90.0	90.0
β, deg	98.09 (1)	90.0	90.0
γ, deg	90.0	90.0	90.0
V, Å^3	2498.7 (7)	2895.4 (9)	3411 (1)
M_r	961.6	1146.7	1331.8
Z	4	4	4
ρ_{calcd}, g/cm^3	2.56	2.63	2.59
	(B) Measurement of Intensity Data		
radiation		Mo Kα (0.71073 Å)	
monochromator		graphite	
detector aperture (mm): horiz; vert		2.0; 2.0	
cryst faces	014, 01$\bar{2}$, 0$\bar{1}$2	0$\bar{1}\bar{1}$, 011, 01$\bar{1}$	$\bar{1}$10, 1$\bar{1}$0, $\bar{1}\bar{1}$0
	01$\bar{2}$, 012, $\bar{1}\bar{1}$1	0$\bar{1}$2, 1$\bar{1}$0, 110	110, 012, 0$\bar{1}\bar{2}$
	11$\bar{1}$, $\bar{1}$1, 1$\bar{1}\bar{1}$	$\bar{1}\bar{1}$0	0$\bar{1}$2, 01$\bar{2}$
cryst size, mm	0.10 × 0.12 × 0.36	0.40 × 0.14 × 0.15	0.09 × 0.24 × 0.224
cryst orientation: direction; deg from ϕ axis	[0$\bar{2}$1]; 0.29	[0$\bar{1}\bar{1}$]; 0.28	[010]; 0.74
reflcns measd	$+h,+k,\pm l$	$+h,+k,+l$	$+h,+k,+l$
scan type		moving cryst–stationary counter	
ω-scan width:[a] $(A + 0.347 \tan \theta)°$		A = 1.1	
bkgd (count time at each end of scan), s		9.0	
ω-scan rate,[a] deg/min		4	
no. of reflcns measd	4962	2901	3058
no. of data used ($F^2 \geq 3.0\sigma(F^2)$)	3023	2482	2296
	(C) Treatment of Data		
abs cor	not applied	not applied	applied
coeff, cm^{-1}	31.03	31.87	31.37
grid			8 × 6 × 8
transmission coeff: max; min			0.82; 0.75
no. of variables (refined)	316	209	242
P factor	0.03	0.03	0.03
final residuals:[b] R_F; R_wF	0.033; 0.036	0.033; 0.039	0.041; 0.044
esd of unit wt observn	1.287	1.435	1.344
largest shift/error value of final cycle	0.03	0.05	0.03
largest peak in final diff Fourier, e/Å^3	0.78	0.77	0.97

[a] Rigaku software uses a multiple-scan technique. If the $I/\sigma(I)$ ratio is less than 10.0, a second scan is made and the results are added to first scan, etc. A maximum of three scans was permitted per reflection. [b] $\sum_{hkl} w(|F_o| - |F_c|)^2$ where $w = 1/\sigma(F)^2$, $\sigma(F) = \sigma(F_o^2)/2F$, and $\sigma(F_o^2) = [\sigma(I_{raw})^2 + (PF_o^2)^2]^{1/2}/Lp$.

and the values of the anisotropic thermal parameters.

Results

The reactions described in this report are summarized in Scheme I. The series of disulfido high-nuclearity clusters $Ru_4(CO)_9(\mu\text{-}CO)_2(\mu_4\text{-}S)_2$ (**3**) (38%), $Ru_5(CO)_{14}(\mu_4\text{-}S)_2$ (**4**) (20%), and $Ru_6(CO)_{17}(\mu_4\text{-}S)_2$ (**5**) (3%) have been obtained from the reaction of $Ru_3(CO)_9(\mu_3\text{-}S)_2$ (**2**) with $Ru_3(CO)_{12}$. Compound **3** was obtained in a much better yield (90%) from the reaction of **2** with $Ru(CO)_5$ in the presence of UV irradiaton.[7] The bis-(dimethylphenylphosphine)-substituted derivative of **3** has been characterized crystallographically.[7] Low solubility in hydrocarbon solvents prevented the study of the reaction of **3** with $Ru(CO)_5$ and probably interfered with the reaction of **3** with $Ru_3(CO)_{12}$ in THF. From the latter reaction low yields of **4** and **5** were obtained. The reaction of **4** with $Ru(CO)_5$ under UV irradiation yielded **5** (24%) and a small amount of $Ru_7(CO)_{20}(\mu_4\text{-}S)_2$ (**6**). Interestingly, **6** was not obtained from irradiated solutions of **5** and $Ru(CO)_5$. The best yield of **6** (26%) was obtained from the pyrolysis of **1** at 100 °C in an evacuated sealed tube. Significant amounts of **3** (47%), **5** (10%), and an unidentified compound **7** were also formed in this reaction.

Compounds **4–6** are broken down by reaction with CO. The major product of these reactions is **3**, which precipitates from the solutions. In CH_2Cl_2, which is a better solvent, **3** reacts quickly with CO at 25 °C to yield **2**.

Compounds **4–6** have been characterized by single-crystal X-ray diffraction analyses. These results are described below.

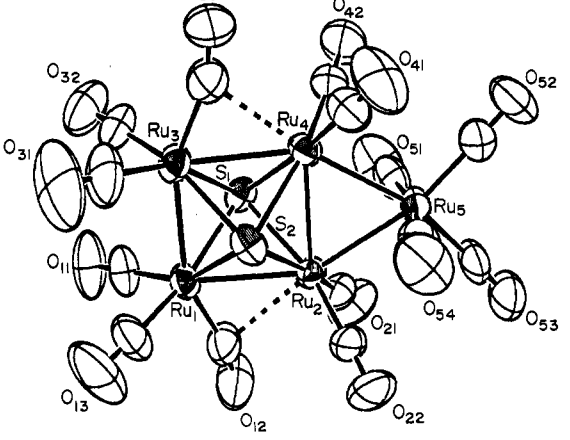

Figure 1. ORTEP diagram of $Ru_5(CO)_{14}(\mu_4\text{-}S)_2$ (**4**) showing 50% probability thermal ellipsoids.

Structure of $Ru_5(CO)_{14}(\mu_4\text{-}S)_2$ (4). An ORTEP diagram of the molecular structure of **4** is shown in Figure 1. Final positional parameters are listed in Table II. Intramolecular distances and bond angles are listed in Tables III and IV, respectively. The molecule consists of an approximately square cluster of four ruthenium atoms with quadruply bridging sulfido ligands positioned on each square face. An $Ru(CO)_4$ group bridges one edge of the

Scheme I

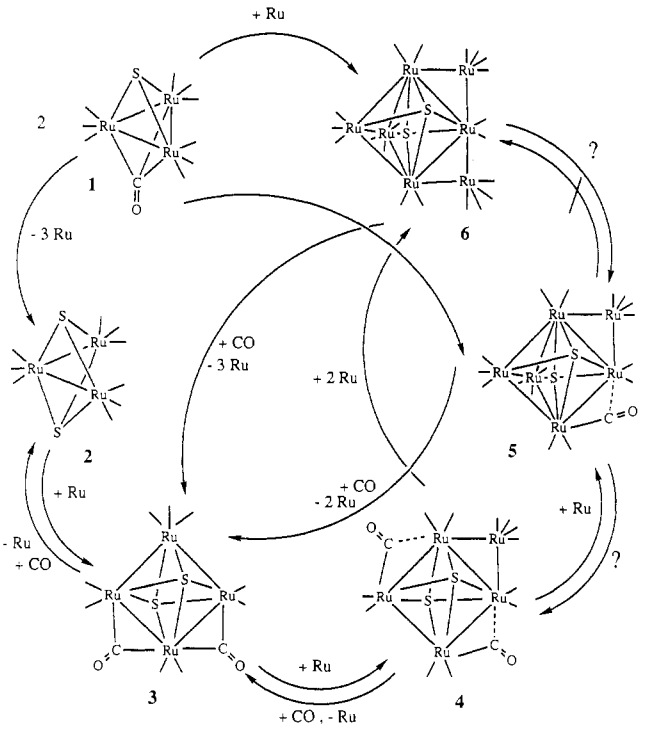

Table II. Positional Parameters and B(eq) for $Ru_5(CO)_{14}(\mu_4\text{-}S)_2$ (**4**)

atom	x	y	z	B(eq), Å^2
Ru1	0.660 695 (75)	0.264 299 (46)	0.478 589 (31)	4.1
Ru2	0.733 097 (67)	0.118 074 (43)	0.400 169 (29)	3.8
Ru3	0.404 552 (81)	0.299 067 (44)	0.389 335 (35)	4.9
Ru4	0.464 481 (71)	0.154 184 (43)	0.307 277 (31)	3.7
Ru5	0.664 077 (81)	0.017 753 (46)	0.283 663 (33)	4.4
S1	0.474 90 (22)	0.144 66 (13)	0.433 919 (97)	4.6
S2	0.658 31 (24)	0.272 65 (14)	0.353 931 (95)	4.2
O11	0.510 2 (12)	0.293 86 (48)	0.604 35 (40)	13.2
O12	0.920 7 (11)	0.156 62 (75)	0.559 23 (43)	12.3
O13	0.830 8 (11)	0.443 76 (63)	0.502 66 (46)	9.4
O21	0.810 15 (85)	−0.054 32 (53)	0.480 50 (39)	11.9
O22	1.060 66 (72)	0.133 64 (57)	0.377 11 (35)	8.2
O31	0.437 1 (15)	0.504 38 (52)	0.383 45 (53)	15.8
O32	0.153 28 (97)	0.314 86 (62)	0.478 91 (45)	12.7
O33	0.168 03 (95)	0.295 54 (54)	0.260 92 (40)	8.8
O41	0.434 0 (12)	0.189 49 (54)	0.157 43 (35)	10.2
O42	0.199 58 (84)	0.025 18 (59)	0.270 96 (46)	7.6
O51	0.471 2 (11)	−0.093 92 (52)	0.372 04 (40)	10.0
O52	0.511 24 (91)	−0.058 73 (55)	0.147 63 (36)	6.8
O53	0.936 36 (96)	−0.112 96 (61)	0.297 66 (40)	9.5
O54	0.839 5 (10)	0.168 87 (63)	0.218 10 (39)	9.9
C11	0.566 5 (13)	0.282 90 (56)	0.557 27 (47)	7.0
C12	0.827 2 (13)	0.189 98 (82)	0.522 72 (54)	7.5
C13	0.769 2 (12)	0.376 18 (76)	0.494 25 (48)	5.7
C21	0.780 2 (10)	0.009 63 (65)	0.449 42 (43)	6.0
C22	0.935 14 (96)	0.126 10 (65)	0.385 75 (39)	5.1
C31	0.422 2 (15)	0.428 50 (73)	0.384 75 (56)	9.8
C32	0.245 7 (12)	0.309 98 (68)	0.444 63 (54)	8.2
C33	0.266 9 (13)	0.284 33 (68)	0.304 34 (52)	7.0
C41	0.448 8 (12)	0.176 52 (59)	0.215 03 (49)	5.7
C42	0.303 3 (11)	0.073 84 (73)	0.285 62 (50)	5.6
C51	0.543 4 (13)	−0.053 28 (62)	0.338 96 (49)	6.0
C52	0.568 8 (11)	−0.031 95 (65)	0.197 79 (50)	5.9
C53	0.832 5 (13)	−0.064 88 (73)	0.291 25 (50)	6.3
C54	0.775 3 (12)	0.113 38 (79)	0.243 55 (46)	6.4

cluster. The metal–metal bonds within the cluster vary considerably. The Ru1–Ru3 distance is unusually short, 2.704 (1) Å. The Ru1–Ru2 and Ru3–Ru4 distances, 2.758 (1) and 2.754 (1) Å, are equal and intermediate in length. The longest bond is Ru2–Ru4, 2.827 (1) Å. The bonds to the edge-bridging $Ru(CO)_4$ group are approximately equal, 2.7195 (9) and 2.732 (1) Å. Although of varying degree, all the Ru–Ru bonds in **4** are shorter than those in $Ru_3(CO)_{12}$, 2.852–2.859 Å.[10] The shape of the cluster of **4** is very similar to that of the bis(dimethylphenylphosphine) derivative of **3**, $Ru_4(CO)_7(\mu\text{-}CO)_2(PMe_2Ph)_2(\mu_4\text{-}S)_2$.[7] The metal–sulfur bonds can be divided into two inequivalent sets.

Table III. Intramolecular Distances (Å) for $Ru_5(CO)_{14}(\mu_4\text{-}S)_2$ (**4**)

Ru1–C11	1.88 (1)	Ru4–S1	2.493 (2)
Ru1–C13	1.89 (1)	Ru4–S2	2.506 (2)
Ru1–C12	1.93 (1)	Ru4–Ru5	2.732 (1)
Ru1–S2	2.461 (2)	Ru5–C53	1.90 (1)
Ru1–S1	2.463 (2)	Ru5–C52	1.92 (1)
Ru1–Ru3	2.704 (1)	Ru5–C51	1.93 (1)
Ru1–Ru2	2.758 (1)	Ru5–C54	1.93 (1)
Ru2–C22	1.841 (8)	O11–C11	1.12 (1)
Ru2–C21	1.87 (1)	O12–C12	1.12 (1)
Ru2–S2	2.481 (2)	O13–C13	1.12 (1)
Ru2–S1	2.483 (2)	O21–C21	1.13 (1)
Ru2–Ru5	2.7195 (9)	O22–C22	1.145 (9)
Ru2–Ru4	2.827 (1)	O31–C31	1.11 (1)
Ru3–C31	1.89 (1)	O32–C32	1.13 (1)
Ru3–C32	1.90 (1)	O33–C33	1.14 (1)
Ru3–C33	1.94 (1)	O41–C41	1.14 (1)
Ru3–S2	2.459 (2)	O42–C42	1.16 (1)
Ru3–S1	2.460 (2)	O51–C51	1.14 (1)
Ru3–Ru4	2.754 (1)	O52–C52	1.12 (1)
Ru4–C41	1.84 (1)	O53–C53	1.14 (1)
Ru4–C42	1.84 (1)	O54–C54	1.14 (1)
Ru2···C12	2.66 (1)	Ru4···C33	2.56 (1)

Table IV. Selected Intramolecular Bond Angles (deg) for $Ru_5(CO)_{14}(\mu_4\text{-}S)_2$ (**4**)

C11–Ru1–Ru3	95.1 (3)	S1–Ru4–Ru3	55.65 (5)
C11–Ru1–Ru2	137.6 (3)	S1–Ru4–Ru2	55.22 (5)
C13–Ru1–Ru3	107.5 (3)	S2–Ru4–Ru5	98.23 (6)
C13–Ru1–Ru2	127.3 (3)	S2–Ru4–Ru3	55.50 (5)
C12–Ru1–Ru3	155.4 (3)	S2–Ru4–Ru2	55.05 (5)
C12–Ru1–Ru2	66.4 (3)	Ru5–Ru4–Ru3	146.82 (3)
S2–Ru1–Ru3	56.63 (5)	Ru5–Ru4–Ru2	58.55 (2)
S2–Ru1–Ru2	56.42 (5)	Ru3–Ru4–Ru2	88.40 (3)
S1–Ru1–Ru3	56.63 (5)	C53–Ru5–Ru2	101.2 (3)
S1–Ru1–Ru2	56.46 (5)	C53–Ru5–Ru4	163.7 (3)
Ru3–Ru1–Ru2	90.87 (3)	C52–Ru5–Ru2	164.8 (3)
C22–Ru2–Ru5	90.5 (2)	C52–Ru5–Ru4	102.3 (3)
C22–Ru2–Ru1	110.0 (3)	C51–Ru5–Ru2	83.3 (3)
C22–Ru2–Ru4	128.6 (3)	C51–Ru5–Ru4	82.8 (3)
C21–Ru2–Ru5	89.6 (3)	C54–Ru5–Ru2	84.0 (3)
C21–Ru2–Ru1	114.3 (3)	C54–Ru5–Ru4	85.5 (3)
C21–Ru2–Ru4	126.7 (3)	Ru2–Ru5–Ru4	62.47 (2)
S2–Ru2–Ru5	99.18 (5)	Ru3–S1–Ru1	66.62 (6)
S2–Ru2–Ru1	55.74 (5)	Ru3–S1–Ru2	103.85 (7)
S2–Ru2–Ru4	55.88 (5)	Ru3–S1–Ru4	67.57 (5)
S1–Ru2–Ru5	101.96 (5)	Ru1–S1–Ru2	67.77 (5)
S1–Ru2–Ru1	55.77 (5)	Ru1–S1–Ru4	104.40 (7)
S1–Ru2–Ru4	55.54 (5)	Ru2–S1–Ru4	69.24 (5)
Ru5–Ru2–Ru1	147.91 (3)	Ru3–S2–Ru1	66.66 (6)
Ru5–Ru2–Ru4	58.98 (2)	Ru3–S2–Ru2	103.94 (7)
Ru1–Ru2–Ru4	89.04 (3)	Ru3–S2–Ru4	67.38 (6)
C31–Ru3–Ru1	98.7 (4)	Ru1–S2–Ru2	67.84 (5)
C31–Ru3–Ru4	135.2 (3)	Ru1–S2–Ru4	104.08 (7)
C32–Ru3–Ru1	104.7 (3)	Ru2–S2–Ru4	69.07 (6)
C32–Ru3–Ru4	128.3 (3)	O11–C11–Ru1	180 (1)
C33–Ru3–Ru1	154.8 (3)	O12–C12–Ru1	167 (1)
C33–Ru3–Ru4	63.5 (3)	O13–C13–Ru1	178 (1)
S2–Ru3–Ru1	56.70 (5)	O21–C21–Ru2	178.2 (9)
S2–Ru3–Ru4	57.12 (5)	O22–C22–Ru2	178.1 (9)
S1–Ru3–Ru1	56.75 (5)	O31–C31–Ru3	178 (1)
S1–Ru3–Ru4	56.78 (5)	O32–C32–Ru3	178 (1)
Ru1–Ru3–Ru4	91.69 (3)	O33–C33–Ru3	161.8 (9)
C41–Ru4–Ru5	85.4 (3)	O41–C41–Ru4	178 (1)
C41–Ru4–Ru3	117.0 (3)	O42–C42–Ru4	178 (1)
C41–Ru4–Ru2	128.0 (3)	O51–C51–Ru5	179 (1)
C42–Ru4–Ru5	89.5 (3)	O52–C52–Ru5	178 (1)
C42–Ru4–Ru3	114.7 (3)	O53–C53–Ru5	177.7 (9)
C42–Ru4–Ru2	125.3 (3)	O54–C54–Ru5	178.1 (9)
S1–Ru4–Ru5	101.36 (5)		

(10) Churchill, M. R.; Hollander, F. J.; Hutchinson, J. P. *Inorg. Chem.* **1977**, *16*, 2655.

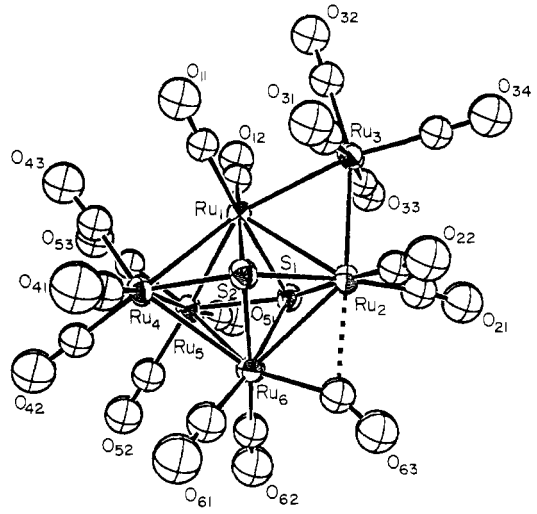

Figure 2. ORTEP diagram of $Ru_6(CO)_{17}(\mu_4\text{-}S)_2$ (**5**) showing 50% probability thermal ellipsoids.

The Ru1–S and Ru3–S distances, 2.459 (2)–2.463 (2) Å, are all shorter than those to Ru2 and Ru4, 2.481 (2)–2.506 (2) Å. Compound **4** has 14 carbonyl ligands. All are of a terminal type, except C12–O12 and C33–O33. These two ligands have semibridging coordination and occupy opposite edges of the cluster, Ru2···C12 = 2.66 (2) Å and Ru4···C33 = 2.56 (2) Å. Overall, the molecule has approximately C_{2v} symmetry. No symmetry is crystallographically imposed.

If one assumes that the sulfido ligands are four-electron donors, then according to the effective atomic number (EAN) rule compound **5** is unsaturated by the amount of two electrons. Such unsaturation could manifest itself in the form of localized multiple bonding, as has been suggested for some structurally similar cluster compounds.[11] Curiously, a simple count of the electron configurations shows that it is the metal atoms Ru2 and Ru4 that formally have the 17-electron configurations, and thus multiple bonding would be expected between these atoms. Surprisingly, the Ru2–Ru4 bond is the longest in the molecule while Ru1–Ru3 is the shortest. This anomaly can be rationalized in the following way. If the Ru1–Ru2 and Ru3–Ru4 bonds are of a donor–acceptor type, Ru1→Ru2 and Ru3→Ru4, then the atoms Ru2 and Ru4 have 18-electron configurations, and Ru1 and Ru3 have 17-electron configurations. The multiple bonding could then occur across the Ru1–Ru3 bond, as in A. The formulation of Ru1–Ru2

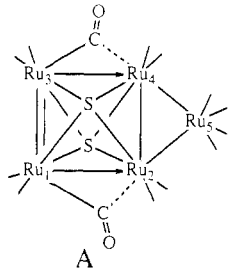

A

and Ru3–Ru4 as donor–acceptor bonds is consistent with one of Cotton's premises concerning the formation of semibridging ligands, as observed in **5**.[12] The total electron count in **5** is 80 electrons. This is the exact number predicted by the well-known delocalized bonding theories.[13]

Structure of $Ru_6(CO)_{17}(\mu_4\text{-}S)_2$ (5). An ORTEP diagram of the molecular structure of **5** is shown in Figure 2. Final positional parameters are listed in Table V. Intramolecular bond distances and angles are listed in Tables VI and VII, respectively. Compound **6** is both isomorphous and isostructural with its osmium homologue.[14] The cluster consists of five ruthenium atoms and

Table V. Positional Parameters and B(eq) for $Ru_6(CO)_{17}(\mu_4\text{-}S)_2$ (**5**)

atom	x	y	z	B(eq), Å^2
Ru1	−0.722 589 (80)	−0.429 243 (60)	−0.195 671 (53)	2.4
Ru2	−0.746 563 (86)	−0.589 024 (63)	−0.098 249 (56)	2.6
Ru3	−0.546 621 (86)	−0.562 078 (67)	−0.184 665 (60)	2.7
Ru4	−0.873 513 (90)	−0.305 879 (67)	−0.107 073 (61)	2.8
Ru5	−0.975 686 (89)	−0.403 622 (68)	−0.228 342 (56)	2.7
Ru6	−0.963 611 (87)	−0.490 874 (70)	−0.077 897 (56)	2.8
S1	−0.879 07 (27)	−0.546 22 (19)	−0.199 84 (17)	2.5
S2	−0.759 96 (27)	−0.432 22 (21)	−0.057 23 (17)	2.7
O11	−0.522 4 (11)	−0.294 25 (78)	−0.183 67 (65)	6.0
O12	−0.694 03 (98)	−0.432 19 (76)	−0.365 08 (60)	5.3
O21	−0.763 4 (11)	−0.788 12 (82)	0.139 21 (63)	6.1
O22	−0.594 0 (10)	−0.636 26 (78)	0.036 31 (66)	5.7
O31	−0.448 8 (10)	−0.455 07 (78)	−0.045 97 (64)	5.7
O32	−0.371 0 (10)	−0.474 28 (75)	−0.294 59 (62)	5.5
O33	−0.677 02 (93)	−0.652 49 (70)	−0.318 53 (61)	4.8
O34	−0.388 2 (11)	−0.726 45 (80)	−0.149 81 (64)	6.0
O41	−0.793 6 (12)	−0.208 98 (95)	0.036 39 (75)	7.5
O42	−1.092 9 (11)	−0.186 76 (87)	−0.105 42 (71)	6.7
O43	−0.752 5 (10)	−0.164 02 (83)	−0.202 17 (66)	6.1
O51	−1.070 3 (11)	−0.508 65 (85)	−0.364 41 (66)	6.3
O52	−1.225 3 (10)	−0.345 73 (80)	−0.191 71 (65)	5.8
O53	−0.928 7 (10)	−0.236 56 (81)	−0.322 03 (69)	6.1
O61	−1.054 8 (12)	−0.395 57 (92)	0.062 99 (75)	7.2
O62	−1.211 4 (12)	−0.553 74 (88)	−0.117 49 (71)	6.8
O63	−0.960 8 (11)	−0.668 63 (78)	0.011 47 (65)	5.8
C11	−0.600 3 (12)	−0.345 61 (91)	−0.187 94 (78)	3.5
C12	−0.706 2 (12)	−0.430 25 (91)	−0.300 37 (75)	3.6
C21	−0.751 4 (14)	−0.709 8 (10)	−0.124 23 (82)	4.5
C22	−0.652 8 (12)	−0.619 67 (90)	−0.014 92 (78)	3.6
C31	−0.486 7 (12)	−0.492 63 (97)	−0.098 29 (83)	3.9
C32	−0.436 1 (13)	−0.509 5 (10)	−0.253 25 (81)	4.3
C33	−0.631 5 (11)	−0.620 13 (84)	−0.268 23 (72)	3.2
C34	−0.451 0 (13)	−0.664 51 (94)	−0.161 59 (74)	3.7
C41	−0.826 4 (14)	−0.247 9 (11)	−0.016 33 (87)	4.6
C42	−1.009 9 (13)	−0.235 29 (95)	−0.109 82 (83)	4.0
C43	−0.796 7 (14)	−0.221 6 (10)	−0.165 96 (82)	4.2
C51	−1.036 9 (13)	−0.469 94 (96)	−0.313 38 (83)	4.0
C52	−1.130 4 (14)	−0.367 7 (10)	−0.204 84 (88)	4.5
C53	−0.944 2 (12)	−0.300 43 (96)	−0.286 17 (74)	3.7
C61	−1.019 9 (14)	−0.431 6 (11)	0.007 98 (93)	4.9
C62	−1.117 2 (14)	−0.528 0 (10)	−0.102 89 (91)	4.5
C63	−0.933 8 (13)	−0.609 3 (10)	−0.024 46 (81)	4.1

Table VI. Intramolecular Distances (Å) for $Ru_6(CO)_{17}(\mu_4\text{-}S)_2$ (**5**)

Ru1–C11	1.84 (1)	Ru5–C51	1.91 (1)
Ru1–C12	1.85 (1)	Ru5–S1	2.408 (3)
Ru1–S1	2.455 (3)	Ru5–Ru6	2.945 (2)
Ru1–S2	2.474 (3)	Ru6–C61	1.86 (2)
Ru1–Ru3	2.779 (1)	Ru6–C62	1.86 (2)
Ru1–Ru2	2.917 (1)	Ru6–C63	2.00 (2)
Ru1–Ru5	2.920 (1)	Ru6–S2	2.467 (3)
Ru1–Ru4	2.928 (1)	Ru6–S1	2.484 (3)
Ru2–C21	1.83 (2)	O11–C11	1.16 (2)
Ru2–C22	1.86 (1)	O12–C12	1.15 (1)
Ru2–S1	2.409 (3)	O21–C21	1.19 (2)
Ru2–S2	2.415 (3)	O22–C22	1.14 (2)
Ru2–Ru3	2.738 (1)	O31–C31	1.15 (2)
Ru2–Ru6	2.850 (1)	O32–C32	1.15 (2)
Ru3–C34	1.89 (1)	O33–C33	1.13 (1)
Ru3–C32	1.89 (1)	O34–C34	1.17 (2)
Ru3–C33	1.95 (1)	O41–C41	1.15 (2)
Ru3–C31	1.95 (1)	O42–C42	1.17 (2)
Ru4–C43	1.83 (2)	O43–C43	1.17 (2)
Ru4–C42	1.85 (1)	O51–C51	1.13 (2)
Ru4–C41	1.89 (2)	O52–C52	1.13 (2)
Ru4–S2	2.413 (3)	O53–C53	1.14 (2)
Ru4–Ru5	2.816 (2)	O61–C61	1.17 (2)
Ru4–Ru6	2.940 (2)	O62–C62	1.15 (2)
Ru5–C53	1.86 (1)	O63–C63	1.12 (2)
Ru5–C52	1.86 (2)	Ru2···C63	2.49 (2)

(11) (a) Vahrenkamp, H.; Wolters, D. *J. Organomet. Chem.* **1982**, *224*, C17. (b) Jaeger, T.; Aime, S.; Vahrenkamp, H. *Organometallics* **1986**, *5*, 245.
(12) Cotton, F. A. *Prog. Inorg. Chem.* **1976**, *21*, 1.
(13) (a) Mingos, D. M. P. *Acc. Chem. Res.* **1984**, *17*, 311. (b) McPartlin, M.; Mingos, D. M. P. *Polyhedron* **1984**, *3*, 1321. (c) Teo, B. K. *Inorg. Chem.* **1984**, *23*, 1257, 1251.

Table VII. Selected Intramolecular Bond Angles (deg) for $Ru_6(CO)_{17}(\mu_4\text{-}S)_2$ (**5**)

C11-Ru1-Ru3	86.2 (4)	C53-Ru5-Ru1	91.6 (4)
C11-Ru1-Ru2	124.0 (4)	C53-Ru5-Ru6	146.9 (4)
C11-Ru1-Ru5	130.6 (4)	C52-Ru5-Ru4	93.8 (5)
C11-Ru1-Ru4	88.8 (4)	C52-Ru5-Ru1	154.1 (5)
C12-Ru1-Ru3	89.6 (4)	C52-Ru5-Ru6	88.0 (5)
C12-Ru1-Ru2	126.0 (4)	C51-Ru5-Ru4	176.9 (4)
C12-Ru1-Ru5	84.4 (4)	C51-Ru5-Ru1	115.9 (4)
C12-Ru1-Ru4	126.3 (4)	C51-Ru5-Ru6	120.0 (4)
S1-Ru1-Ru3	91.12 (8)	S1-Ru5-Ru4	95.80 (8)
S1-Ru1-Ru2	52.43 (8)	S1-Ru5-Ru1	53.84 (7)
S1-Ru1-Ru5	52.37 (7)	S1-Ru5-Ru6	54.16 (8)
S1-Ru1-Ru4	91.99 (8)	Ru4-Ru5-Ru1	61.36 (3)
S2-Ru1-Ru3	92.24 (8)	Ru4-Ru5-Ru6	61.33 (4)
S2-Ru1-Ru2	52.45 (8)	Ru1-Ru5-Ru6	73.87 (3)
S2-Ru1-Ru5	91.83 (8)	C61-Ru6-Ru2	129.0 (5)
S2-Ru1-Ru4	52.26 (8)	C61-Ru6-Ru4	80.0 (5)
Ru3-Ru1-Ru2	57.40 (3)	C61-Ru6-Ru5	120.9 (5)
Ru3-Ru1-Ru5	142.54 (4)	C62-Ru6-Ru2	127.8 (5)
Ru3-Ru1-Ru4	143.73 (5)	C62-Ru6-Ru4	123.2 (5)
Ru2-Ru1-Ru5	97.46 (4)	C62-Ru6-Ru5	82.6 (5)
Ru2-Ru1-Ru4	97.45 (4)	C63-Ru6-Ru2	58.6 (4)
Ru5-Ru1-Ru4	57.57 (3)	C63-Ru6-Ru4	145.6 (4)
C21-Ru2-Ru3	91.4 (5)	C63-Ru6-Ru5	143.8 (4)
C21-Ru2-Ru6	119.7 (5)	S2-Ru6-Ru2	53.45 (8)
C21-Ru2-Ru1	129.3 (5)	S2-Ru6-Ru4	52.12 (8)
C22-Ru2-Ru3	90.6 (4)	S2-Ru6-Ru5	91.36 (8)
C22-Ru2-Ru6	120.4 (4)	S1-Ru6-Ru2	53.16 (7)
C22-Ru2-Ru1	127.3 (4)	S1-Ru6-Ru4	91.11 (7)
S1-Ru2-Ru3	93.12 (8)	S1-Ru6-Ru5	51.81 (7)
S1-Ru2-Ru6	55.61 (8)	Ru2-Ru6-Ru4	98.67 (4)
S1-Ru2-Ru1	53.88 (7)	Ru2-Ru6-Ru5	98.37 (4)
S2-Ru2-Ru3	94.57 (8)	Ru4-Ru6-Ru5	57.16 (3)
S2-Ru2-Ru6	55.14 (8)	Ru5-S1-Ru2	131.2 (1)
S2-Ru2-Ru1	54.32 (8)	Ru5-S1-Ru1	73.79 (9)
Ru3-Ru2-Ru6	134.11 (5)	Ru5-S1-Ru6	74.02 (9)
Ru3-Ru2-Ru1	58.78 (3)	Ru2-S1-Ru1	73.7 (1)
Ru6-Ru2-Ru1	75.34 (4)	Ru2-S1-Ru6	71.2 (1)
C34-Ru3-Ru2	103.3 (4)	Ru1-S1-Ru6	91.1 (1)
C34-Ru3-Ru1	167.1 (4)	Ru4-S2-Ru2	130.9 (1)
C32-Ru3-Ru2	161.5 (4)	Ru4-S2-Ru6	74.1 (1)
C32-Ru3-Ru1	97.7 (4)	Ru4-S2-Ru1	73.6 (1)
C33-Ru3-Ru2	87.5 (4)	Ru2-S2-Ru6	71.42 (9)
C33-Ru3-Ru1	84.7 (4)	Ru2-S2-Ru1	73.23 (9)
C31-Ru3-Ru2	85.6 (4)	Ru6-S2-Ru1	91.0 (1)
C31-Ru3-Ru1	86.2 (4)	O11-C11-Ru1	179 (1)
Ru2-Ru3-Ru1	63.82 (3)	O12-C12-Ru1	179 (1)
C43-Ru4-Ru5	96.1 (5)	O21-C21-Ru2	175 (1)
C43-Ru4-Ru1	81.0 (5)	O22-C22-Ru2	178 (1)
C43-Ru4-Ru6	152.2 (5)	O31-C31-Ru3	177 (1)
C42-Ru4-Ru5	85.9 (4)	O32-C32-Ru3	177 (1)
C42-Ru4-Ru1	144.2 (5)	O33-C33-Ru3	177 (1)
C42-Ru4-Ru6	103.7 (4)	O34-C34-Ru3	177 (1)
C41-Ru4-Ru5	170.5 (5)	O41-C41-Ru4	176 (1)
C41-Ru4-Ru1	124.6 (5)	O42-C42-Ru4	174 (1)
C41-Ru4-Ru6	111.4 (5)	O43-C43-Ru4	176 (1)
S2-Ru4-Ru5	95.72 (8)	O51-C51-Ru5	178 (1)
S2-Ru4-Ru1	54.16 (8)	O52-C52-Ru5	179 (1)
S2-Ru4-Ru6	53.79 (8)	O53-C53-Ru5	178 (1)
Ru5-Ru4-Ru1	61.07 (4)	O61-C61-Ru6	179 (1)
Ru5-Ru4-Ru6	61.51 (4)	O62-C62-Ru6	178 (1)
Ru1-Ru4-Ru6	73.83 (4)	O63-C63-Ru6	154 (1)
C53-Ru5-Ru4	85.6 (4)		

two sulfido ligands arranged in the form of a pentagonal bipyramid. An $Ru(CO)_4$ group bridges an apical–equatorial edge, Ru1–Ru2 of the cluster. The apical–equatorial metal–metal and metal–sulfur bond distances are longer than the equatorial–equatorial metal–metal and metal–sulfur distances. Application of the EAN rule would suggest that the Ru2–Ru6 bond is a donor–acceptor metal–metal bond, Ru6→Ru2, and as might be expected, this bond contains an appropriately positioned semibridging carbonyl ligand: Ru2···C63 = 2.49 (2) Å, Ru6–C63–O63 = 154 (1)°.[12] The principal difference between **5** and the osmium homologue is that, except for one bond (Ru1–Ru5) that is identical in length with that in the osmium compound, all the metal–metal bonds in **5** are shorter, 0.01–0.05 Å, than those in the osmium compound. Compound **5** contains a total of 94 valence electrons and obeys both the EAN rule and the delocalized bonding theories.[13]

Table VIII. Positional Parameters and B(eq) for $Ru_7(CO)_{20}(\mu_4\text{-}S)$ (**6**)

atom	x	y	z	B(eq), Å^2
Ru1	1.94592 (14)	1.54450 (11)	1.419300 (71)	3.11 (7)
Ru2	1.73897 (13)	1.437688 (96)	1.387632 (70)	2.79 (7)
Ru3	1.88802 (15)	1.38256 (11)	1.484947 (72)	3.52 (7)
Ru4	1.85015 (15)	1.72970 (10)	1.400591 (72)	3.28 (7)
Ru5	1.96708 (15)	1.64456 (11)	1.298636 (74)	3.48 (7)
Ru6	1.71759 (14)	1.606542 (97)	1.315185 (64)	2.59 (6)
Ru7	1.54379 (15)	1.46940 (12)	1.311049 (79)	3.69 (8)
S1	1.88087 (43)	1.49273 (31)	1.31356 (22)	3.1 (2)
S2	1.73754 (41)	1.59254 (31)	1.43007 (20)	2.8 (2)
O11	2.0258 (18)	1.6344 (13)	1.54024 (88)	8.0 (5)
O12	2.1947 (16)	1.4749 (12)	1.39585 (84)	7.1 (4)
O21	1.7615 (14)	1.2483 (11)	1.32886 (76)	6.2 (4)
O22	1.5577 (16)	1.3671 (12)	1.48067 (79)	6.7 (4)
O31	2.0326 (15)	1.2792 (11)	1.38401 (75)	6.3 (4)
O32	1.7535 (17)	1.5120 (13)	1.57525 (83)	7.5 (4)
O33	1.7775 (20)	1.2040 (16)	1.5369 (10)	9.9 (6)
O34	2.0986 (19)	1.3810 (15)	1.57103 (98)	9.5 (6)
O41	2.0805 (16)	1.8364 (12)	1.41008 (88)	7.5 (5)
O42	1.7647 (19)	1.7923 (14)	1.5302 (10)	8.7 (5)
O43	1.7251 (17)	1.8938 (13)	1.34202 (83)	7.7 (5)
O51	1.9193 (15)	1.8356 (13)	1.24565 (82)	7.0 (4)
O52	2.0435 (18)	1.5658 (13)	1.17143 (89)	8.4 (5)
O53	2.2224 (16)	1.6778 (12)	1.32883 (80)	6.7 (4)
O61	1.7248 (14)	1.6219 (11)	1.17277 (75)	6.0 (4)
O62	1.5193 (14)	1.7481 (11)	1.31947 (77)	6.2 (4)
O71	1.6924 (13)	1.3890 (11)	1.20109 (71)	5.6 (3)
O72	1.3829 (20)	1.5722 (15)	1.2208 (10)	9.7 (6)
O73	1.4364 (15)	1.5717 (11)	1.42413 (74)	6.2 (4)
O74	1.3827 (22)	1.3027 (17)	1.3251 (12)	11.3 (7)
C11	1.9947 (22)	1.5972 (18)	1.4901 (12)	6.2 (6)
C12	2.0986 (21)	1.5018 (16)	1.4043 (11)	4.9 (5)
C21	1.7486 (19)	1.3208 (15)	1.35172 (98)	4.3 (4)
C22	1.6273 (21)	1.3973 (16)	1.4445 (10)	5.1 (5)
C31	1.9780 (20)	1.3195 (15)	1.4206 (10)	4.5 (5)
C32	1.8053 (20)	1.4674 (16)	1.5389 (10)	4.9 (5)
C33	1.8200 (24)	1.2730 (20)	1.5164 (13)	6.7 (6)
C34	2.0168 (25)	1.3827 (19)	1.5398 (12)	6.6 (6)
C41	1.9929 (21)	1.7914 (15)	1.4042 (11)	5.0 (5)
C42	1.8013 (26)	1.7711 (21)	1.4818 (14)	7.3 (7)
C43	1.7734 (21)	1.8313 (16)	1.3664 (10)	5.2 (5)
C51	1.9395 (21)	1.7609 (16)	1.2667 (11)	5.2 (5)
C52	2.0108 (22)	1.5939 (18)	1.2200 (12)	6.0 (6)
C53	2.1233 (22)	1.6667 (16)	1.3169 (11)	5.3 (5)
C61	1.7227 (18)	1.6154 (14)	1.22787 (90)	3.8 (4)
C62	1.5959 (18)	1.6929 (14)	1.31728 (98)	3.9 (4)
C71	1.6408 (19)	1.4173 (15)	1.24293 (98)	4.5 (4)
C72	1.4391 (23)	1.5309 (18)	1.2559 (12)	6.4 (6)
C73	1.4797 (18)	1.5323 (14)	1.38249 (94)	4.2 (4)
C74	1.4422 (28)	1.3680 (21)	1.3197 (14)	8.0 (7)

Structure of $Ru_7(CO)_{20}(\mu_4\text{-}S)_2$ (6). An ORTEP diagram of the molecular structure of **6** is shown in Figure 3. Final positional parameters are listed in Table VIII. Intramolecular bond distances and angles are listed in Tables IX and X, respectively. Compound **6**, like **5**, is isomorphous and isostructural with its osmium homologue. The structure of $Os_7(CO)_{20}(\mu_4\text{-}S)_2$ has been reported.[15] The cluster of **6** is very similar to that of **5** and consists of a pentagonal-bipyramidal cluster of five ruthenium atoms and two sulfido ligands. $Ru(CO)_4$ groups bridge the Ru1–Ru2 and Ru2–Ru6 apical–equatorial edges of the cluster. The principal difference between **6** and the osmium homologue is that all the metal–metal bonds in **6** are shorter, 0.01–0.04 Å, than those in the osmium compound. All the metal atoms in **6** obey the EAN rule. Compound **6** with 108 valence electrons also adheres to the

(14) Adams, R. D.; Horvath, I. T.; Yang, L. W. *J. Am. Chem. Soc.* **1983**, *105*, 1533.

(15) Adams, R. D.; Horvath, I. T.; Mathur, P.; Segmuller, B. E.; Yang, L. W. *Organometallics* **1983**, *2*, 1078.

Table IX. Intramolecular Distances (Å) for $Ru_7(CO)_{20}(\mu_4\text{-}S)_2$ (**6**)

Ru1–C11	1.77 (3)	Ru6–C62	1.84 (2)
Ru1–C12	1.85 (2)	Ru6–C61	1.86 (2)
Ru1–S1	2.449 (5)	Ru6–S2	2.453 (5)
Ru1–S2	2.473 (5)	Ru6–S1	2.456 (5)
Ru1–Ru3	2.782 (2)	Ru6–Ru7	2.770 (2)
Ru1–Ru2	2.862 (2)	Ru7–C74	1.85 (3)
Ru1–Ru4	2.889 (2)	Ru7–C72	1.88 (3)
Ru1–Ru5	2.943 (2)	Ru7–C73	1.90 (2)
Ru2–C22	1.83 (2)	Ru7–C71	1.96 (2)
Ru2–C21	1.84 (2)	O11–C11	1.24 (3)
Ru2–S2	2.373 (5)	O12–C12	1.16 (2)
Ru2–S1	2.393 (5)	O21–C21	1.16 (2)
Ru2–Ru7	2.765 (2)	O22–C22	1.18 (2)
Ru2–Ru3	2.772 (2)	O31–C31	1.15 (2)
Ru2–Ru6	2.875 (2)	O32–C32	1.16 (2)
Ru3–C34	1.86 (3)	O33–C33	1.18 (3)
Ru3–C33	1.87 (3)	O34–C34	1.13 (3)
Ru3–C32	1.91 (2)	O41–C41	1.18 (2)
Ru3–C31	1.92 (2)	O42–C42	1.15 (3)
Ru4–C41	1.83 (2)	O43–C43	1.17 (2)
Ru4–C43	1.84 (2)	O51–C51	1.18 (2)
Ru4–C42	1.90 (3)	O52–C52	1.17 (3)
Ru4–S1	2.418 (5)	O53–C53	1.15 (3)
Ru4–Ru5	2.809 (2)	O61–C61	1.17 (2)
Ru4–Ru6	2.934 (2)	O62–C62	1.17 (2)
Ru5–C53	1.82 (2)	O71–C71	1.14 (2)
Ru5–C51	1.82 (2)	O72–C72	1.14 (3)
Ru5–C52	1.88 (3)	O73–C73	1.16 (2)
Ru5–S2	2.401 (5)	O74–C74	1.16 (3)
Ru5–Ru6	2.875 (2)		

delocalized cluster bonding theories.[13]

Discussion

In this report we have described the synthesis and characterization of the new higher nuclearity disulfido ruthenium carbonyl clusters **4**–**6** as well as the previously known cluster **3** from condensation reactions of the triruthenium cluster compounds **1** and **2**; see Scheme I. The series **3**–**6** differ in sequence by the amount of one ruthenium atom. It seems most likely that they are formed by the sequential addition of mononuclear ruthenium carbonyl fragments formed in situ to each of the clusters **2**–**4**. The additions are difficult to control. The reactions give product mixtures, and the yields are not good. We have not been able to obtain **6** by addition of a mononuclear ruthenium fragment to **5**. Likewise, we were unable to prepare the osmium homologue of **6** by addition of a mononuclear osmium fragment to the osmium homologue of **5**. The formation of **6** apparently occurs by cluster growth a

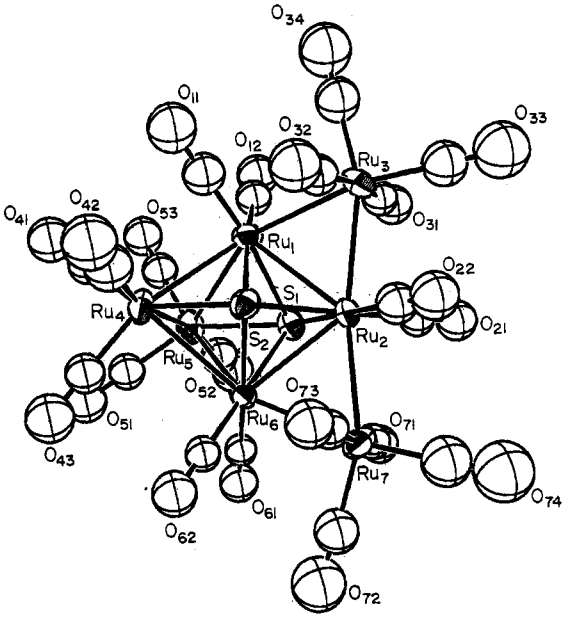

Figure 3. ORTEP diagram of $Ru_7(CO)_{20}(\mu_4\text{-}S)_2$ (**6**) showing 50% probability thermal ellipsoids.

Table X. Selected Intramolecular Bond Angles (deg) for $Ru_7(CO)_{20}(\mu_4\text{-}S)_2$ (**6**)

C11–Ru1–Ru3	90.2 (8)	S1–Ru2–Ru6	54.6 (1)	C52–Ru5–Ru4	166.1 (7)	C73–Ru7–Ru6	84.6 (6)
C11–Ru1–Ru2	132.8 (8)	Ru7–Ru2–Ru3	164.27 (8)	C52–Ru5–Ru6	106.8 (8)	C71–Ru7–Ru2	86.0 (6)
C11–Ru1–Ru4	80.8 (8)	Ru7–Ru2–Ru1	133.91 (7)	C52–Ru5–Ru1	127.1 (8)	C71–Ru7–Ru6	84.4 (6)
C11–Ru1–Ru5	120.4 (8)	Ru7–Ru2–Ru6	58.78 (5)	S2–Ru5–Ru4	95.9 (1)	Ru2–Ru7–Ru6	62.59 (5)
C12–Ru1–Ru3	91.6 (7)	Ru3–Ru2–Ru1	59.16 (6)	S2–Ru5–Ru6	54.5 (1)	Ru2–S1–Ru4	130.7 (2)
C12–Ru1–Ru2	122.4 (7)	Ru3–Ru2–Ru6	133.47 (7)	S2–Ru5–Ru1	54.0 (1)	Ru2–S1–Ru1	72.4 (1)
C12–Ru1–Ru4	128.7 (7)	Ru1–Ru2–Ru6	75.15 (5)	Ru4–Ru5–Ru6	62.15 (5)	Ru2–S1–Ru6	72.7 (1)
C12–Ru1–Ru5	86.3 (7)	C34–Ru3–Ru2	159.5 (8)	Ru4–Ru5–Ru1	60.25 (6)	Ru4–S1–Ru1	72.8 (1)
S1–Ru1–Ru3	88.0 (1)	C34–Ru3–Ru1	97.6 (8)	Ru6–Ru5–Ru1	73.92 (5)	Ru4–S1–Ru6	74.0 (1)
S1–Ru1–Ru2	52.9 (1)	C33–Ru3–Ru2	105.0 (8)	C62–Ru6–Ru7	87.4 (6)	Ru1–S1–Ru6	91.0 (2)
S1–Ru1–Ru4	53.1 (1)	C33–Ru3–Ru1	167.0 (8)	C62–Ru6–Ru5	126.7 (6)	Ru2–S2–Ru5	131.2 (2)
S1–Ru1–Ru5	91.2 (1)	C32–Ru3–Ru2	88.4 (7)	C62–Ru6–Ru2	127.8 (6)	Ru2–S2–Ru6	73.1 (1)
S2–Ru1–Ru3	97.8 (1)	C32–Ru3–Ru1	83.3 (7)	C62–Ru6–Ru4	87.6 (6)	Ru2–S2–Ru1	72.4 (1)
S2–Ru1–Ru2	52.2 (1)	C31–Ru3–Ru2	85.5 (6)	C61–Ru6–Ru7	92.2 (6)	Ru5–S2–Ru6	72.6 (1)
S2–Ru1–Ru4	92.3 (1)	C31–Ru3–Ru1	85.0 (6)	C61–Ru6–Ru5	80.5 (6)	Ru5–S2–Ru1	74.3 (1)
S2–Ru1–Ru5	51.7 (1)	Ru2–Ru3–Ru1	62.02 (5)	C61–Ru6–Ru2	126.0 (6)	Ru6–S2–Ru1	90.5 (2)
Ru3–Ru1–Ru2	58.82 (5)	C41–Ru4–Ru5	80.4 (7)	C61–Ru6–Ru4	124.0 (6)	O11–C11–Ru1	178 (2)
Ru3–Ru1–Ru4	138.33 (8)	C41–Ru4–Ru1	96.4 (7)	S2–Ru6–Ru7	93.1 (1)	O12–C12–Ru1	179 (2)
Ru3–Ru1–Ru5	149.32 (8)	C41–Ru4–Ru6	139.4 (7)	S2–Ru6–Ru5	52.8 (1)	O21–C21–Ru2	176 (2)
Ru2–Ru1–Ru4	98.99 (7)	C43–Ru4–Ru5	105.0 (7)	S2–Ru6–Ru2	52.1 (1)	O22–C22–Ru2	177 (2)
Ru2–Ru1–Ru5	96.98 (6)	C43–Ru4–Ru1	162.6 (7)	S2–Ru6–Ru4	91.7 (1)	O31–C31–Ru3	177 (2)
Ru4–Ru1–Ru5	57.56 (5)	C43–Ru4–Ru6	89.7 (7)	S1–Ru6–Ru7	92.2 (1)	O32–C32–Ru3	174 (2)
C22–Ru2–Ru7	84.1 (7)	C42–Ru4–Ru5	165.3 (9)	S1–Ru6–Ru5	92.7 (1)	O33–C33–Ru3	179 (3)
C22–Ru2–Ru3	80.4 (7)	C42–Ru4–Ru1	105.6 (9)	S1–Ru6–Ru2	52.6 (1)	O34–C34–Ru3	177 (2)
C22–Ru2–Ru1	124.7 (7)	C42–Ru4–Ru6	126.9 (9)	S1–Ru6–Ru4	52.4 (1)	O41–C41–Ru4	174 (2)
C22–Ru2–Ru6	124.1 (7)	S1–Ru4–Ru5	95.2 (1)	Ru7–Ru6–Ru5	144.76 (7)	O42–C42–Ru4	175 (3)
C21–Ru2–Ru7	87.3 (7)	S1–Ru4–Ru1	54.1 (1)	Ru7–Ru6–Ru2	58.63 (5)	O43–C43–Ru4	177 (2)
C21–Ru2–Ru3	90.8 (7)	S1–Ru4–Ru6	53.6 (1)	Ru7–Ru6–Ru4	143.42 (7)	O51–C51–Ru5	179 (2)
C21–Ru2–Ru1	122.4 (7)	Ru5–Ru4–Ru1	62.19 (6)	Ru5–Ru6–Ru2	98.23 (6)	O52–C52–Ru5	176 (2)
C21–Ru2–Ru6	123.2 (6)	Ru5–Ru4–Ru6	60.03 (6)	Ru5–Ru6–Ru4	57.82 (5)	O53–C53–Ru5	178 (2)
S2–Ru2–Ru7	95.1 (1)	Ru1–Ru4–Ru6	73.85 (6)	Ru2–Ru6–Ru4	97.64 (6)	O61–C61–Ru6	179 (2)
S2–Ru2–Ru3	100.5 (1)	C53–Ru5–Ru4	102.1 (8)	C74–Ru7–Ru2	107 (1)	O62–C62–Ru6	179 (2)
S2–Ru2–Ru1	55.4 (1)	C53–Ru5–Ru6	160.7 (8)	C74–Ru7–Ru6	170 (1)	O71–C71–Ru7	176 (2)
S2–Ru2–Ru6	54.7 (1)	C53–Ru5–Ru1	88.7 (8)	C72–Ru7–Ru2	159.9 (8)	O72–C72–Ru7	175 (2)
S1–Ru2–Ru7	93.6 (1)	C51–Ru5–Ru4	79.1 (7)	C72–Ru7–Ru6	97.4 (8)	O73–C73–Ru7	177 (2)
S1–Ru2–Ru3	89.3 (1)	C51–Ru5–Ru6	93.0 (7)	C73–Ru7–Ru2	84.8 (6)	O74–C74–Ru7	177 (3)
S1–Ru2–Ru1	54.7 (1)	C51–Ru5–Ru1	138.9 (7)				

stage prior to the formation of **5**. Compound **5** was obtained by the thermal decarbonylation and condensation of 2 mol of **1**. $Os_6(CO)_{17}(\mu_4\text{-}S)_2$ was prepared in good yield by the photoinduced decarbonylation and condensation of 2 mol of $Os_3(CO)_9(\mu_3\text{-}CO)(\mu_3\text{-}S)$.[16] Interestingly, $Os_6(CO)_{17}(\mu_4\text{-}S)_2$ can be decarbonylated to form the more highly condensed species $Os_6(CO)_{16}(\mu_4\text{-}S)(\mu_3\text{-}S)$.[14] We found no evidence for this reaction with **5**. Instead, when compound **5** was heated, the cluster broke down and compound **3** was formed.

The greatest differences in structural chemistry between the disulfidoruthenium and the disulfidoosmium carbonyl cluster series lie in compounds **3** and **4**. $Os_4(CO)_{11}(\mu_4\text{-}S)_2$ has not yet been prepared. $Os_4(CO)_{12}(\mu_3\text{-}S)_2$ is known, but it has a butterfly tetrahedral cluster of metal atoms.[17] Our efforts to decarbonylate $Os_4(CO)_{12}(\mu_3\text{-}S)_2$ to form $Os_4(CO)_{11}(\mu_4\text{-}S)_2$ have not been successful.[18] Interestingly, we have been able to transform the butterfly clusters $Os_4(CO)_{12}(\mu_3\text{-}S)(\mu_3\text{-}HC_2R)$ (R = Ph, CO_2Me) into the square clusters $Os_4(CO)_{11}(\mu_4\text{-}S)(\mu_4\text{-}HC_2R)$.[19] To date, there are no known examples of disulfidopentaosmium carbonyl clusters with which to compare to **4**.

Another difference between the two series lies in their reactivities toward CO. The ruthenium clusters are readily degraded under 1 atm of CO to give either **3** as a precipitate or **2**. The osmium compounds are much more resistant to degradation by CO. For example, $Os_6(CO)_{16}(\mu_4\text{-}S)(\mu_3\text{-}S)$ does not react significantly when treated with CO at 165 atm/210 °C for 2 days. This difference in reactivity can probably be attributed to the greater strength of the Os–Os vs. the Ru–Ru bonds.[20] Most CO addition reactions induce metal–metal bond cleavages.

Acknowledgment. The research was supported by the National Science Foundation under Grant No. CHE-8612862.

Registry No. **1**, 105121-22-0; **2**, 72282-38-3; **3**, 105121-25-3; **4**, 109433-55-8; **5**, 109433-54-7; **6**, 109466-69-5; $Ru_3(CO)_{12}$, 15243-33-1; $Ru(CO)_5$, 16406-48-7.

Supplementary Material Available: For compounds **4–6**, tables of complete bond angles and of anisotropic thermal parameters (U values) (15 pages); listings of structure factor amplitudes (54 pages). Ordering information is given on any current masthead page.

(16) Adams, R. D.; Horvath, I. T.; Kim, H. S. *Organometallics* **1984**, *3*, 548.
(17) Adams, R. D.; Yang, L. W. *J. Am. Chem. Soc.* **1983**, *105*, 235.
(18) Adams, R. D.; Wang, S., unpublished results.
(19) Adams, R. D.; Wang, S. *J. Am. Chem. Soc.* **1987**, *109*, 924.
(20) Connor, J. A. In *Transition Metal Clusters*; Johnson, B. F. G., Ed.; Wiley: Chichester, England, 1980; Chapter 5.

Contribution from the Institute of Inorganic Chemistry, University of Fribourg, Pérolles, CH-1700 Fribourg, Switzerland

Cyclometalated Complexes of Platinum(II): Homoleptic Compounds with Aromatic C,N Ligands

L. Chassot and A. von Zelewsky*

Received September 12, 1986

The synthesis of the five new homoleptic bis(cyclometalated) Pt(II) complexes *cis*-Pt(Phpz)$_2$ (II, $C_{18}H_{14}N_4Pt$), *cis*-Pt(Thpy)$_2$ (III, $C_{18}H_{12}N_2S_2Pt$), Pt(3-Thpy)$_2$ (IV, $C_{18}H_{12}N_2S_2Pt$), *cis*-Pt(Thpy-SiMe$_3$)$_2$ (V, $C_{24}H_{28}N_2S_2Si_2Pt$), and *cis*-Pt(Thpz)$_2$ (VI, $C_{14}H_{10}N_4S_2Pt$) from *trans*-$PtCl_2(SEt_2)_2$ and the lithiated ligands at low temperature (−78 °C) is described. All compounds are air-stable, soluble in many organic solvents, and photoreactive in solution under irradition with visible light. The strong low-energy bands in the electronic spectra in the range from 400 to 450 nm are assigned to metal to ligand charge-transfer (MLCT) transitions from a Pt(5d) orbital to an empty π^* orbital of the ligands. Most spectra show a weak absorption superimposed on the low-energy side of the strong MLCT band. This weak absorption is attributed to a singlet–triplet transition of the same type as the strong band. The complexes can be reduced electrochemically in reversible one-electron steps. Oxidation occurs also, but in a completely irreversible manner.

Introduction

Cyclometalated complexes represent a link between classic, Werner-type coordination compounds and organometallic species.[1] We are exploring presently the possibility of synthesizing *homoleptic* complexes with C,N aromatic cycles of several transition metals.[2] Such species are promising candidates for interesting photochemical and photophysical properties.[3] The first example of a homoleptic bis complex with aromatic ligands of a d^8 metal was described recently.[4] In the present paper, we describe further examples in the series. The platinum(II) complexes I–VI are characterized by using several analytical methods.

All these compounds are air stable and they can be crystallized from several solvents. In some cases precautions, during the handling of solutions, against photoreactions have to be taken.

The synthesis, X-ray crystal structure, and several properties of I have already been published; some results have not yet been given, however. In this report I is included for the sake of completeness.

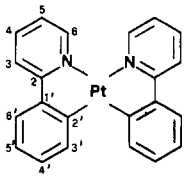

I

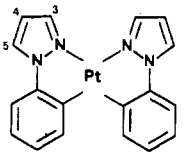

II

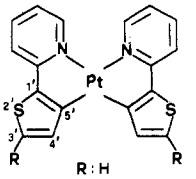

R : H
III

R : $Si(CH_3)_3$
V

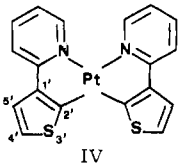

IV

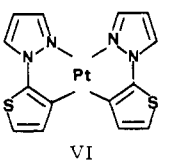

VI

Experimental Section

Measurements. Electronic spectra were recorded with a Perkin-Elmer 555 spectrophotometer. ^1H NMR spectra were collected with Varian T-60, Varian XL-300, and Bruker M-360 spectrometers. ^{13}C NMR spectra were obtained on Varian XL-300 and Bruker M-360 spectrometers at 75.5 and 90.6 MHz. Natural-abundance ^{195}Pt NMR spectra were obtained on a Bruker M-360 spectrometer with a wide-bore (20-mm) probe at 70.07 MHz (external reference $Pt(CN)_6^{2-}$ in H_2O). Mass

(1) Constable, E. C. *Polyhedron* **1984**, *3*, 1037.
(2) Chassot, L Ph.D. Thesis University of Fribourg 1985.
(3) Maestri, M.; Sandrini, D.; Balzani, V.; Chassot, L.; Jolliet, Ph.; von Zelewsky, A. *Chem. Phys. Lett.* **1985**, *122*, 375. Bonafede, S.; Ciano, M.; Bolletta, F.; Balzani, V.; Chassot, L.; von Zelewsky, A. *J. Phys. Chem.* **1986**, *90*, 3836. Chassot, L.; von Zelewsky, A.; Sandrini, D.; Maestri, M.; Balzani, V. *J. Am. Chem. Soc.* **1986**, *108*, 6084.
(4) Chassot, L.; Mueller, E.; von Zelewsky, A. *Inorg. Chem.* **1984**, *23*, 4249.

0020-1669/87/1326-2814$01.50/0